JACS
JOURNAL OF THE AMERICAN CHEMICAL SOCIETY

Communication

pubs.acs.org/JACS

Structural Insight into NS5 of Zika Virus Leading to the Discovery of MTase Inhibitors

Preyesh Stephen,[†] Mariana Baz,[‡] Guy Boivin,[‡] and Sheng-Xiang Lin*[,†]

[†]Axe Molecular Endocrinology and Nephrology, CHU Research Center and Department of Molecular Medicine, Laval University, Québec City, Québec G1V 4G2, Canada

[‡]Axe Infectious Disease, CHU Research Center and Laval University, Québec City, Québec G1V 4G2, Canada

Supporting Information

ABSTRACT: Zika virus (ZIKV) is an emerging mosquito-borne virus recently linked to intrauterine growth restriction including abnormal fetal brain development. The recent outbreak of ZIKV reached pandemic level resulting in an alarming public health emergency. At present, there is limited understanding of the infectious mechanism and no approved therapy. Nonstructural protein 5 is essential for capping and replication of viral RNA and comprises a methyltransferase (MTase) and RNA dependent RNA polymerase domain. Here we used molecular modeling to obtain the structure of ZIKV MTase and molecular docking to identify the additional hydrophobic region uniquely conserved in flavivirus MTase that can be used as a druggable site. Subsequently, a virtual screening with a library of 28 341 compounds identified 10 best hits showing decisive contacts with the MTase. In vitro efficacy analysis of these compounds against ZIKV, by plaque reduction assay, has confirmed four of the top scored ligands (Life Chemicals ID: F3043-0013, F0922-0796, F1609-0442, and F1750-0048) having EC50 (50% effective concentration) values of 4.8 ± 2.3, 12.5 ± 7.4, 17.5 ± 8.4, and 17.6 ± 3.1 μM respectively, identifying lead compounds for anti-ZIKV drug development.

Zika virus (ZIKV) infection underlies a recent epidemic that has spread in South and Central America and the Caribbean with a recent report of locally acquired cases in Florida and Singapore. ZIKV is an *Aedes* mosquito-transmitted flavivirus, which has recently been linked to a serious birth defect of the brain called microcephaly and other poor pregnancy outcomes in babies of infected mothers. Recent studies confirmed that the ZIKV can cross the placental barrier and enter the amniotic fluid during pregnancy.[1] Moreover, case studies of ZIKV association to microcephaly in newborns[2−4] strengthen the evidence for the involvement of ZIKV in microcephaly. Whereas ZIKV infection is primarily a vector-borne transmission, recent reports of probable non-vector-borne transmissions[1,5] reveal the potential for pandemic spread.[6] Despite the increased potential of ZIKV, there is currently no available antiviral therapy. A recent study reported the identification of compounds that showed the ability to hinder the progress of ZIKV in human neural cells.[7] However, there are no understanding on solubility, drug-target mechanism, and in vivo reactions, which are necessary for any drug to rush into clinics. The recent outbreak and the need to understand the infection mechanism underlie the urgency to design multidimensional strategies to tackle ZIKV, before it becomes a serious pandemic.

The ZIKV genome is located inside the capsid and contains a single-stranded positive sense RNA molecule of 10 794 kb in length consisting of 2 flanking noncoding regions (5′ and 3′ NCR) and an open reading frame encoding a polyprotein.[8] The polyprotein consists of seven nonstructural proteins (NS), which plays an important role in RNA replication.[9] Nonstructural protein 5 (NS5, ∼103 kDa) is the largest and most conserved viral protein consisting of an N-terminal RNA capping domain with methyl transferase activity (MTase) and a C-terminal RNA-dependent RNA polymerase (RdRp) domain.[10]

Remarkable attempts of NS5-based drug design in flaviviruses targeted MTase[11,12] and RdRp.[13−15] Novel nucleotide analogs targeting ZIKV RdRp were proposed recently,[16] and extensive preclinical studies must be carried out before these data can be translated to clinical trials. Metal binding pocket of RdRp and SAH/SAM (*S*-adenosyl-L-homocysteine/*S*-adenosyl-L-methionine) binding pocket of MTase are conventionally used in drug screening. Additional targeting sites are proposed in NS5, such as the residues important for NS3−NS5 interaction[17] essential for the virus replication.

Flavivirus MTase has a conserved hydrophobic cavity adjacent to the SAH/SAM binding pocket.[18] Absence of this conserved hydrophobic binding pocket in human N7/2′O MTase motivated us to design inhibitors targeting this pocket. Though the crystal structure of ZIKV MTase has been resolved,[19] there was no ZIKV MTase crystal structure available during the initiation of this project. Thus, we modeled the three-dimensional structure of MTase by using Modeler 9.14 based on template structure of Modoc virus (MODV; PDB ID: 2WA1). The MODV MTase is the only crystal structure without a bound ligand available in the PDB. Steepest Descent method from SwissPDB viewer was used for energy minimization. A series of structure validation programs were used to verify the modeled structure. The modeled structure is now deposited in PMDB database, with PMDB ID PM0080437.

Received: October 4, 2016
Published: November 28, 2016

DOI: 10.1021/jacs.6b10399
J. Am. Chem. Soc. 2016, 138, 16212−16215

The modeled ZIKV NS5 is identical to the crystal structure recently published,[19] containing 43 α-helices and 20 β-sheets (Figure 1A, Figure S1). An overlap of the modeled MTase

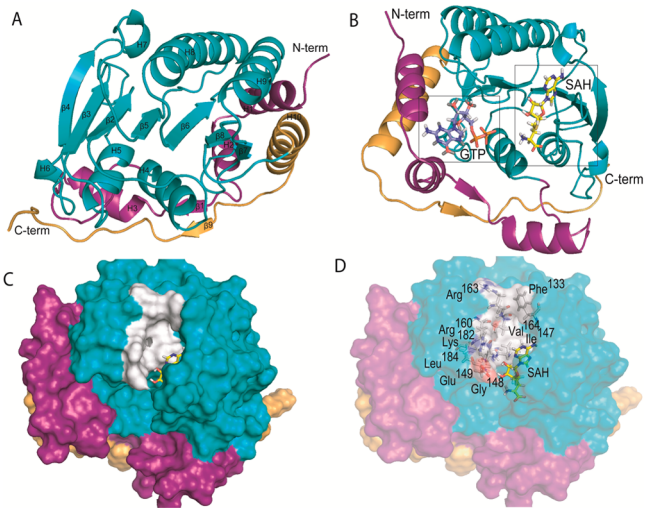

Figure 1. (A) Ribbon representation of modeled ZIKV MTase structure. The structural core, N-terminal, and C-terminal are colored in cyan, purple, and orange, respectively. α-Helices and β-sheets are numbered. (B) Location and binding pose of SAH (yellow) and GTP (blue) in ZIKV MTase are shown. (C) Surface representation of ZIKV MTase. SAH is shown in sticks representation in yellow color. The additional hydrophobic cavity near the SAH binding pocket is colored in white. (D) Corresponding amino acids involved in the additional pocket are labeled and shown in a stick representation, with white color.

structure to the ZIKV crystal structure (PDB ID: 5KQR) gave an RMSD below 0.9 Å, showing negligible differences. ZIKV NS5 is a large protein that is structurally conserved among members of the genus, containing an MTase domain and an RNA dependent RNA polymerase (RdRp) domain, which are connected by a 10 residue linker (265AVASCAEAPN275).

The cofactor SAM is the methyl donor in flaviviruses that transfers the methyl group to the enzyme substrate and is converted to *S*-adenosyl homocysteine (SAH). We used the program SwissDock to obtain a ZIKV MTase SAH complex, and the genetic algorithm GOLD[21] to obtain ZIKV MTase GTP complex (Figure 1B). For the SAH complex, 20 docked poses were manually analyzed, after a blind docking that uses the vicinity of the target cavities of the entire protein surface. In ZIKV MTase, SAH is stretched between H7 and the loop between H3 and H4. A binding pocket is mainly formed by residues in loops extending from β2−5 and H5 holding the SAH by 9 hydrogen bonds and 5 hydrophobic contacts. The residues demonstrated to interact with SAH in our docking analysis were congruent with binding sites demonstrated in crystal structure.[19] A serious concern in targeting the SAM binding pocket is the strong affinity of SAM to flavivirus MTases, which means it may be difficult to design inhibitors that can out-compete the bound SAM inside the cell.

Mutational studies in dengue viruses have demonstrated a hydrophobic cavity near the SAM binding pocket, where amino acid mutations impaired the methylation.[18] This hydrophobic cavity in ZIKV MTase is spreading through β6, H7, H8, and the loop connecting β5 to H8 and β8 and H9. Phe^{133}, Ile^{147}, Gly^{148}, Glu^{149}, Arg^{160}, Arg^{163}, Val^{164}, Lys^{182}, and Leu^{184} are the hydrophobic residues spanning in this region of ZIKV MTase (Figure 1C,D). An inhibitor screening exploiting this hydrophobic cavity in addition to the large SAM binding pocket will accelerate the quest for lead molecules with improved specificity and selectivity.

A virtual screening of 28 341 compounds from Life Chemicals database was carried out using GOLD version 5.4.1. Ten Ångstroms around Val^{164} was defined as the binding pocket. This was to derive the best possible conformers utilizing the hydrophobic region near to SAM binding pocket. The best 10 ligands were chosen based on the scores obtained from the ChemPLP and verifying with the genetic docking algorithm GOLD (Table S1). However, compounds with higher ChemPLP but significantly lower GOLD score are omitted. GOLD score is based on H-bonding energy, van der Waals energy, metal interaction, and ligand torsion strain, whereas ChemPLP uses the hydrogen bonding term and multiple linear potentials to model van der Waals and repulsive terms. ChemPLP is the default and in general the best performing scoring function for both pose prediction and virtual screening. Nevertheless, the scores between different scoring functions cannot be compared directly. The druglikeness of the compounds is not tested, but the compounds in the Life Chemicals library has already been passed through the Lipinsky's rule of five, Veber criteria, and dissimilarity evaluation. All the best 10 compounds ranked in screening are soluble in DMSO, but solubility in any other solvents is not known. Molecular masses of the best 10 compounds are listed in Table 1 to facilitate the idea that the smaller the better for the diffusion of the drug.

Table 1. EC50 Calculation of Best 10 Compounds by PRA

product ID	[a]MM (da)	ChemPLP	GOLD score	EC50 (μM)
F3043-0013	526	93	66	4.8 ± 2.3
F0922-0796	588	94	44	12.5 ± 7.4
F1609-0442	507	93	50	17.5 ± 8.4
F1750-0048	564	92	56	17.6 ± 3.1
F1604-0217	460	92	51	>25
F0590-0267	492	97	50	>25
F0922-0375	572	95	46	>25
F1601-0134	485	94	44	>25
F0922-0372	568	94	53	>25
F1602-0599	571	98	53	>25

[a]MM = Molecular mass.

Interestingly, the best scored compounds showed ChemPLP scores higher than the natural substrates. Docking of SAM and SAH to 10 Å around amine group of Gly144 gave ChemPLPs as 62 and 79, respectively. The top scored 10 compounds listed in Table 1 have ChemPLP scores of 92−98. A strong interaction by the inhibitor molecule is expected to out-compete the bound SAM inside the cell. The binding pocket of the best scored compounds partially covers the hydrophobic pocket and extends to the SAM binding pocket.

Plaque reduction assay (PRA), a gold standard phenotypic method for in vitro efficacy analysis was carried out by treating each of the 10 compounds against ZIKV isolated from a Canadian traveler in 2013.[20] The confluent cells were seeded in 6-well plates with 30−50 plaque forming units (PFUs) and incubated for 90 min at 37 °C in a 5% CO_2 atm. Triplicate wells of infected cells were then incubated for 5 days with 2-fold serial dilutions of each compound (ranging from 3.9 to 50 μM) in Minimum Essential Medium with 2% fetal bovine

DOI: 10.1021/jacs.6b10399
J. Am. Chem. Soc. 2016, 138, 16212−16215

serum containing 0.6% SeaPlaque agarose. Cells were then fixed and stained, and the number of PFUs was counted under an inverted microscope (Figure 2). Determination of 50% effective concentration (EC50) of the compounds was based on PFU of each PRA. Compounds showing EC50 > 25 μM are not taken for further studies.

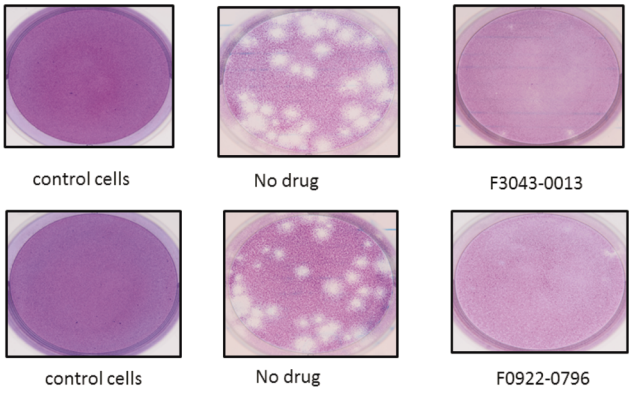

Figure 2. Plaque reduction assay performed using Vero cells for compounds F3043-0013 and F0922-0796 showing the inhibition of ZIKV at 25 μM of each antiviral drug after 5 days of incubation at 37 °C in the absence or presence of the drug.

Table 1 shows the EC50 obtained for the 10 best compounds. F3043-0013 [chemical name: 2-(4-((4-phenylpiperazin-1-yl)sulfonyl)phenethyl)-1H-benzo[de]isoquinoline-1,3(2H)-dione], F0922-0796 [chemical name: 4-((1-(2-((3,4-dimethoxyphenethyl)amino)-2-oxoethyl)-2,4-dioxo-1,4-dihydroquinazolin-3(2H)-yl)methyl)-*N*-(3-methoxypropyl)benzamide], F1609-0442 [chemical name: 2-(3-benzoyl-6-methyl-4-oxoquinolin-1(4H)-yl)-*N*-(o-tolyl)acetamide], and F1750-0048 [chemical name: 4-((3,4-dihydroisoquinolin-2(1H)-yl)sulfonyl)-*N*-(4-(N-(4-methylpyrimidin-2-yl)sulfamoyl)phenyl)benzamide] have EC50 values of 4.8 ± 2.3, 12.5 ± 7.4, 17.5 ± 8.4, and 17.6 ± 3.1 μM, respectively. EC50 values obtained for these compounds show better potential than other ZIKV lead molecules in the literature, except that obtained for 2′-*C*-methyladenosine: EC50 value of 5.26 μM.[16]

The binding potency of these ligands is facilitated by cooperative interactions at hydrophobic binding pocket, extending to the SAH binding pocket. A detailed report of protein−ligand contacts demonstrated by the best 4 lead molecules is shown in Table 2.

The inhibitor F3043-0013, which showed the best EC50 of 4.8 ± 2.3 μM, is a ring containing structure (Figure 3A) having

Table 2. Polar and Hydrophobic Interactions Established between the Lead Molecules and the MTase

product ID	polar interaction	hydrophobic interactions
F3043-0013	Gly^{148}	Ser^{56}, Gly^{81}, Cys^{82}, Gly^{83}, Arg^{84}, Gly^{85}, Gly^{86}, Thr^{104}, Lys^{105}, Glu^{111}, Asp^{131}, Val^{132}, Phe^{133}, Ile^{147}, Arg^{160}, Arg^{163}, Val^{164}
F0922-0796	Cys^{82}, Arg^{84}	Ser^{56}, Gly^{81}, Gly^{83}, Gly^{85}, Gly^{86}, Thr^{104}, Lys^{105}, His^{110}, Glu^{111}, Val^{130}, Asp^{131}, Val^{132}, Phe^{133}, Asp^{146}, Ile^{147}, Thr^{159}, Arg^{160}, Arg^{163}, Val^{164}
F1750-0048	Lys105, Val132, Gly77	Ser^{56}, Arg^{57}, Gly^{58}, Lys^{61}, Gly^{83}, Arg^{84}, His^{110}, Asp^{131}, Phe^{133}, Asp^{146}, Ile^{147}, Arg^{163}, Val^{164}
F1609-0442	Lys105	Thr^{104}, Lys^{105}, Glu^{111}, Asp^{131}, Val^{132}, Phe^{133}, Ile^{147}, Gly^{148}, Arg^{163}, Val^{164}

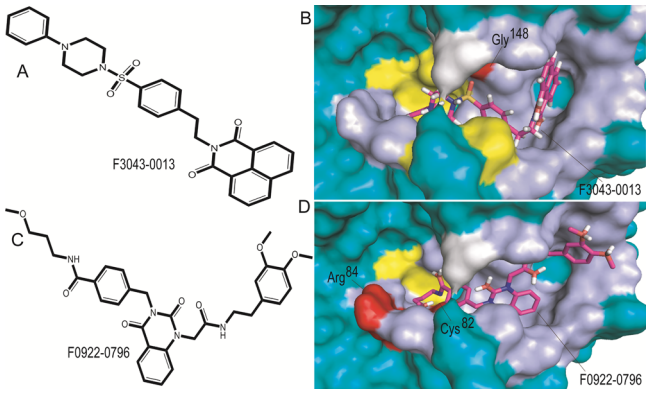

Figure 3. Chemical structures of F3043-0013 (A) and F0922-0796 (C) and docked complexes of F3043-0013 (B) and F0922-0796 (D) in the binding pocket of MTase. MTase is represented as surface and colored in cyan. Ligands are represented as sticks with magenta color and labeled. Noninteracting amino acids in SAH and the additional hydrophobic binding pocket are colored in yellow and white, respectively. Amino acids involved in hydrogen bonds and hydrophobic interactions with the ligands are colored in red and light-blue, respectively.

molecular mass of 526 g/mol and log *P* value of 5.11. The ChemPLP score (93) and GOLD score (66) were reasonably higher with ample contacts established by the ligand with the binding pocket in MTase. Interactions by 17 hydrophobic residues (Ser^{56}, Gly^{81}, Cys^{82}, Gly^{83}, Arg^{84}, Gly^{85}, Gly^{86}, Thr^{104}, Lys^{105}, Glu^{111}, Asp^{131}, Val^{132}, Phe^{133}, Ile^{147}, Arg^{160}, Arg^{163}, and Val^{164}) are further reinforced by a hydrogen bond through the amino group of Gly^{148} and double bond oxygen on sulfur in F3043-0013 (Figure 3B, Table 2). Worthy to note, mutating Gly^{148}Ala abolished both the N-7 as well as the 2′-O methylation capacity of the Dengue MTase. Arg^{160}, Arg^{163} are important in N-7 methylation and Phe^{133} is important in 2′-O methylation.[18]

The second best ligand was F0922-0796, which showed an EC50 of 12.5 ± 7.4 μM and the highest ChemPLP score (98). F0922-0796 is also a ring containing structure (Figure 3C) with molecular mass of 588 g/mol and log *P* value of 2.3. The strong interaction by F0922-0796 with MTase is established through 19 hydrophobic amino acids (Ser^{56}, Gly^{81}, Gly^{83}, Gly^{85}, Gly^{86}, Thr^{104}, Lys^{105}, His^{110}, Glu^{111}, Val^{130}, Asp^{131}, Val^{132}, Phe^{133}, Asp^{146}, Ile^{147}, Thr^{159}, Arg^{160}, Arg^{163}, and Val^{164}) and two hydrogen bonding amino acids (Cys^{82}, Arg^{84}) (Figure 3D, Table 2). Hydrogen bonds are formed by N3 and O7 of F0922-0796 with carboxyl oxygen of Cys^{82} and side chain amino group of Arg^{84}, respectively.

Various amino acids involved in contacts with top scored ligands are also shown to interact with SAH, indicating these inhibitor−MTase contacts may take place when the ligand can out-compete SAH. The additional contacts established with hydrophobic cleft by these ligands will support them to out-compete SAM/SAH.

Three out of the seven mutations reported in the ZIKV MTase domain[21] are situated near the hydrophobic binding pocket (Figure S2). However, *in silico* mutations in the MTase structure modified neither the native conformation nor the interactions with surrounding amino acids. Thus, such mutational changes may only have a negligible impact on the efficacy of these proposed molecules.

In summary, using a structure-guided approach, we have demonstrated potential lead molecules for ZIKV selective

DOI: 10.1021/jacs.6b10399
J. Am. Chem. Soc. 2016, 138, 16212−16215

inhibition by taking advantage of the flavivirus specific hydrophobic pocket in MTases. The proposed lead compounds will be further tested in rodent models for therapy of ZIKV infection. Additionally, the significant inhibition of MTase by our leads confirms the high precision of our model, and predicts the methodological value in other virus pandemics.

■ ASSOCIATED CONTENT

Supporting Information

The Supporting Information is available free of charge on the ACS Publications website at DOI: 10.1021/jacs.6b10399.

Experimental procedures and supporting tables, and supporting figure (PDF)

■ AUTHOR INFORMATION

Corresponding Author

*sxlin@crchul.ulaval.ca

ORCID

Sheng-Xiang Lin: 0000-0001-9149-375X

Notes

The authors declare no competing financial interest.

■ ACKNOWLEDGMENTS

S.-X.L. acknowledges financial support from Quebec CHU Foundation (No. 2759) and CIHR Foundation. G.B. acknowledges financial support from CIHR Foundation (No. 148361).

■ REFERENCES

(1) Calvet, G.; Aguiar, R. S.; Melo, A. S.; Sampaio, S. A.; de Filippis, I.; Fabri, A.; Araujo, E. S.; de Sequeira, P. C.; de Mendonca, M. C.; de Oliveira, L.; Tschoeke, D. A.; Schrago, C. G.; Thompson, F. L.; Brasil, P.; Dos Santos, F. B.; Nogueira, R. M.; Tanuri, A.; de Filippis, A. M. *Lancet Infect. Dis.* **2016**, *16*, 653.

(2) de Araujo, T. V.; Rodrigues, L. C.; de Alencar Ximenes, R. A.; de Barros Miranda-Filho, D.; Montarroyos, U. R.; de Melo, A. P.; Valongueiro, S.; de Albuquerque, M. F.; Souza, W. V.; Braga, C.; Filho, S. P.; Cordeiro, M. T.; Vazquez, E.; Di Cavalcanti Souza Cruz, D.; Henriques, C. M.; Bezerra, L. C.; da Silva Castanha, P. M.; Dhalia, R.; Marques-Junior, E. T.; Martelli, C. M. *Lancet Infect. Dis.* **2016**, *16*, 1356.

(3) Martines, R. B.; Bhatnagar, J.; Keating, M. K.; Silva-Flannery, L.; Muehlenbachs, A.; Gary, J.; Goldsmith, C.; Hale, G.; Ritter, J.; Rollin, D.; Shieh, W. J.; Luz, K. G.; Ramos, A. M.; Davi, H. P.; Kleber de Oliveria, W.; Lanciotti, R.; Lambert, A.; Zaki, S. *MMWR Morb Mortal Wkly Rep* **2016**, *65*, 159.

(4) Mlakar, J.; Korva, M.; Tul, N.; Popovic, M.; Poljsak-Prijatelj, M.; Mraz, J.; Kolenc, M.; Resman Rus, K.; Vesnaver Vipotnik, T.; Fabjan Vodusek, V.; Vizjak, A.; Pizem, J.; Petrovec, M.; Avsic Zupanc, T. *N. Engl. J. Med.* **2016**, *374*, 951.

(5) Musso, D.; Roche, C.; Robin, E.; Nhan, T.; Teissier, A.; Cao-Lormeau, V. M. *Emerging Infect. Dis.* **2015**, *21*, 359.

(6) Lucey, D. R.; Gostin, L. O. *JAMA* **2016**, *315*, 865.

(7) Xu, M.; Lee, E. M.; Wen, Z.; Cheng, Y.; Huang, W. K.; Qian, X.; Tcw, J.; Kouznetsova, J.; Ogden, S. C.; Hammack, C.; Jacob, F.; Nguyen, H. N.; Itkin, M.; Hanna, C.; Shinn, P.; Allen, C.; Michael, S. G.; Simeonov, A.; Huang, W.; Christian, K. M.; Goate, A.; Brennand, K. J.; Huang, R.; Xia, M.; Ming, G. L.; Zheng, W.; Song, H.; Tang, H. *Nat. Med.* **2016**, *22*, 1101.

(8) Chambers, T. J.; Hahn, C. S.; Galler, R.; Rice, C. M. *Annu. Rev. Microbiol.* **1990**, *44*, 649.

(9) Nulf, C. J.; Corey, D. *Nucleic Acids Res.* **2004**, *32*, 3792.

(10) Lindenbach, B. D.; Rice, C. M. *Adv. Virus Res.* **2003**, *59*, 23.

(11) Chung, K. Y.; Dong, H.; Chao, A. T.; Shi, P. Y.; Lescar, J.; Lim, S. P. *Virology* **2010**, *402*, 52.

(12) Stahla-Beek, H. J.; April, D. G.; Saeedi, B. J.; Hannah, A. M.; Keenan, S. M.; Geiss, B. J. *J. Virol.* **2012**, *86*, 8730.

(13) Nguyen, N. M.; Tran, C. N.; Phung, L. K.; Duong, K. T.; Huynh, H. A.; Farrar, J.; Nguyen, Q. T.; Tran, H. T.; Nguyen, C. V.; Merson, L.; Hoang, L. T.; Hibberd, M. L.; Aw, P. P.; Wilm, A.; Nagarajan, N.; Nguyen, D. T.; Pham, M. P.; Nguyen, T. T.; Javanbakht, H.; Klumpp, K.; Hammond, J.; Petric, R.; Wolbers, M.; Nguyen, C. T.; Simmons, C. P. *J. Infect. Dis.* **2013**, *207*, 1442.

(14) Smith, T. M.; Lim, S. P.; Yue, K.; Busby, S. A.; Arora, R.; Seh, C. C.; Wright, S. K.; Nutiu, R.; Niyomrattanakit, P.; Wan, K. F.; Beer, D.; Shi, P. Y.; Benson, T. E. *J. Biomol. Screening* **2015**, *20*, 153.

(15) Xu, H. T.; Colby-Germinario, S. P.; Hassounah, S.; Quashie, P. K.; Han, Y.; Oliveira, M.; Stranix, B. R.; Wainberg, M. A. *Antimicrob. Agents Chemother.* **2016**, *60*, 600.

(16) Eyer, L.; Nencka, R.; Huvarova, I.; Palus, M.; Joao Alves, M.; Gould, E. A.; De Clercq, E.; Ruzek, D. *J. Infect. Dis.* **2016**, *214*, 707.

(17) Zhao, Y.; Soh, T. S.; Chan, K. W.; Fung, S. S.; Swaminathan, K.; Lim, S. P.; Shi, P. Y.; Huber, T.; Lescar, J.; Luo, D.; Vasudevan, S. G. *J. Virol.* **2015**, *89*, 10717.

(18) Lim, S. P.; Sonntag, L. S.; Noble, C.; Nilar, S. H.; Ng, R. H.; Zou, G.; Monaghan, P.; Chung, K. Y.; Dong, H.; Liu, B.; Bodenreider, C.; Lee, G.; Ding, M.; Chan, W. L.; Wang, G.; Jian, Y. L.; Chao, A. T.; Lescar, J.; Yin, Z.; Vedananda, T. R.; Keller, T. H.; Shi, P. Y. *J. Biol. Chem.* **2011**, *286*, 6233.

(19) Coloma, J.; Jain, R.; Rajashankar, K. R.; García-Sastre, A.; Aggarwal, A. K. *Cell Rep.* **2016**, *16*, 6.

(20) Fonseca, K.; Meatherall, B.; Zarra, D.; Drebot, M.; MacDonald, J.; Pabbaraju, K.; Wong, S.; Webster, P.; Lindsay, R.; Tellier, R. *Am. J. Trop. Med. Hyg.* **2014**, *91*, 1035.

(21) Baez, C. F.; Barel, V. A.; de Souza, A. M.; Rodrigues, C. R.; Varella, R. B.; Cirauqui, N. *Mol. BioSyst.* **2016**, DOI: 10.1039/C6MB00645K.

DOI: 10.1021/jacs.6b10399
J. Am. Chem. Soc. 2016, 138, 16212−16215